UHASSELT
KNOWLEDGE IN ACTION

Maastricht University

# Faculty of Medicine and Life Sciences
## *School for Life Sciences*
## Master of Biomedical Sciences

***Master's thesis***

***The influence of microplastics on the human intestine: an in vitro study on uptake and transport under different exposure conditions***

**Daphne Schraepen**

Thesis presented in fulfillment of the requirements for the degree of Master of Biomedical Sciences, specialization Environmental Health Sciences

**SUPERVISOR :**

dr. Nelly SAENEN

**2020**
**2021**

Transnational University Limburg is a unique collaboration of two universities in two countries: the University of Hasselt and Maastricht University.

UHASSELT
KNOWLEDGE IN ACTION

**www.uhasselt.be**
Universiteit Hasselt
Campus Hasselt:
Martelarenlaan 42 | 3500 Hasselt
Campus Diepenbeek:
Agoralaan Gebouw D | 3590 Diepenbeek

UHASSELT
KNOWLEDGE IN ACTION

Maastricht University

# Faculty of Medicine and Life Sciences
## *School for Life Sciences*
## Master of Biomedical Sciences

***Master's thesis***

***The influence of microplastics on the human intestine: an in vitro study on uptake and transport under different exposure conditions***

**Daphne Schraepen**

Thesis presented in fulfillment of the requirements for the degree of Master of Biomedical Sciences, specialization Environmental Health Sciences

**SUPERVISOR :**

dr. Nelly SAENEN

# The influence of microplastics on the human intestine: an *in vitro* study of uptake and transport under different exposure conditions*

Daphne Schraepen[1], Msc. Margo Witters[1], Dr. Nelly Saenen[1] and Prof. Dr. Karen Smeets[1]

[1]Zoology, biodiversity, and toxicology research group, Centre for Environmental Sciences, Hasselt University, Agoralaan Building D,3590 Diepenbeek, Belgium

*Running title: *In vitro uptake and transport of microplastics*

To whom correspondence should be addressed: Karen Smeets, Tel: +32 11 26 83 19; Email: karen.smeets@uhasselt.be

**Keywords:** Polystyrene microplastics - Gastrointestinal barrier - Caco-2 cells - Characterisation - Cellular uptake - Endocytosis

## ABSTRACT

**Nowadays, microplastics are an omnipresent environmental pollutant. They are small enough to be ingested by humans directly or via consumption of, for example, contaminated (sea)food. Consequently, microplastics enter the gastrointestinal tract and interact with the intestinal epithelium. To develop a basic scientific understanding about this interaction, several *in vitro* studies have been conducted. However, current data on microplastic uptake and transport is inconclusive due to variations in experimental approach and lack of fundamental understanding. This study aims to provide an overview of the effects of different exposure conditions on the uptake and transport of Polystyrene microplastics *in vitro*. Human epithelial Caco-2 cells, and a co-culture with HT29-MTX cells, were exposed to carboxylated Polystyrene spheres (200 nm or 2 µm). After physicochemical characterisation, uptake and transport were evaluated using FACS, confocal microscopy, and fluorescence intensity measurements. Our data show that MPs are taken up and transported by Caco-2 cells. In addition, they suggest that the presence of serum proteins in cell medium causes a reduction in uptake (up to 36%). We found a trend towards increased uptake for longer exposure durations and smaller microplastic size. Lastly, an effect of cell model was observed. Further differentiation of the cells negatively affected uptake, and the presence of mucus reduced transport to less than half. These results indicate that caution should be taken when comparing and interpreting research data as varying exposure conditions significantly affect microplastic uptake and transport across a Caco-2 monolayer. However, additional research is necessary to fill in remaining knowledge gaps.**

## INTRODUCTION

Plastic has become ubiquitous in the modern world. Since the start of its production in the 1950s, plastic usage has increased more than three hundred-fold (1, 2). The most abundant polymer types include Polyethylene (PE), Polypropylene (PP), and Polystyrene (PS). They account for the majority of plastic waste found in aquatic environments (3). Larger plastic pieces are widely studied in relation to entanglement and digestive tract congestion (4, 5). However, smaller plastics, such as microplastics (MPs) (<5 mm), are possibly even more dangerous (6). Since researchers are only at the start of the scientific discovery regarding MPs, a fundamental understanding of the consequences their presence might have on the environment as well as human health is still limited (7-9). In a recent report, EFSA stated that information on plastic particle uptake kinetics is still insufficient for a reliable risk assessment (6).

Some MPs, called primary MPs, are intentionally manufactured on the microscale. They have a wide range of applications in medical, pharmaceutical, industrial, and cosmetic fields, and are therefore of great interest (10). Secondary MPs

originate from larger plastic debris that is degraded by environmental factors such as UV radiation, ocean waves etc. As such, plastics occur in a variety of shapes and sizes, including spheres, fibres, and fragments (11). These physicochemical characteristics have been shown to significantly affect MP uptake and transport in living cells (12). Both primary and secondary MPs often end up in the environment. They may be taken up by aquatic organisms and pollute drinking water. Hence, they can enter the food chain and cause human exposure (13).

The oral route is considered one of the main exposure routes for humans. It has been shown that the average person ingests up to 100 000 plastic particles yearly via diet or inhalation (11). Not only contamination from packaging, like plastic bottles or tubs, but also consumption results in exposure. Seafood, drinking water, salt, beer, and even teabags contain a vast amount of MPs (14-18). Schwabl *et al*. demonstrated the presence of MPs in human stool samples, proving exposure via ingestion (19).

Current studies dealing with MP exposure mainly focus on polystyrene (PS) spheres (10, 20-22). The popularity of PS in human exposure research is due to its environmental abundance, well-defined characteristics, relatively low cost, and the wide variety of commercially available PS MPs (23). This synthetic polymer is often used in food containers and disposable cutlery. Fiorentino and colleagues already proved the uptake of 44 nm PS plastics by primary human cell cultures (24). Additionally, *in vivo* research showed transfer of PS microspheres from the GI-tract to the circulation after oral ingestion in rats (25).

Because of the wide variety of MP types and sizes, it is not feasible to routinely assess the safety of MPs via *in vivo* models. Consequently, alternative testing methods to reduce animal studies are becoming increasingly important due to societal demand (10). For this purpose, an immortalized cell line of human epithelial colorectal adenocarcinoma cells, called Caco-2 cells, can be applied (26, 27). The Caco-2 monolayer model is well-established and has been shown to simulate the human intestinal barrier effectively (28). However, scientific literature on MP uptake and transport is controversial due to the inconsistent use of exposure conditions and techniques. Some papers assess MP exposure in serum-free medium (29, 30), while others add foetal bovine serum (FBS) to the cell medium (10, 20, 22). Occasionally, a study uses limited exposure durations of 10 - 120 min (20), but prolonged exposures of 24 - 96 h are applied as well (21, 26, 31). Additionally, MP sizes ranging from 25 nm to 6 µm and more are studied (26, 32, 33). The effect of this variety in experimental set-ups remains unclear.

**In this study, we aim to enhance the interpretation of MP research by providing coherent and fundamental information on the effect of different exposure conditions on MP uptake and transport in an *in vitro* intestinal model.** First, we focus on characterising the MPs. Next, we assess uptake in different exposure conditions. The effect of variations in exposure duration, FBS addition, MP size, and stage of cell differentiation on MP uptake will be compared using multiple techniques. In addition, we perform a pilot study to determine the role of active transport by analysing the consequences of blocking (caveolae-mediated) endocytosis. Finally, we compare transport across a Caco-2 monoculture and a Caco-2 HT29-MTX co-culture to determine the influence of mucus on MP transport across the monolayer. In summary, this research focuses on providing the knowledge necessary to create more coherent and representative research on the effects of MPs in intestinal model systems.

## EXPERIMENTAL PROCEDURES

*Microplastics*

Carboxyl-modified, red fluorescently labelled (Ex/: 530/590) PS spheres of two different sizes (200 nm, and 2 µm) were purchased from Magsphere (Pasadena, USA). In the further course of this paper, the 200 nm MPs will be referred to as PS200-RF and the 2 µm MPs as PS2-RF. Detailed information provided by the manufacturer is described in Table 1. The sizes were chosen to represent submicron and micron scale. Stock solutions of 1 mg/ml were prepared in Milli-Q and sterilized with gamma irradiation at 30 Gy. All suspensions were stored at 4°C. Before experiments, the PS MPs were further diluted in the relevant medium.

**Table 1: Specifications of the PS microplastics as provided by the manufacturer.**

| ID | Diameter ± SD (µm) | % Solids | Polymer Density (g/ml) | Fluorescent Dye Contents (%w/w) | Surface Groups | Surfactant | Em/Ex Wavelength (nm) |
|---|---|---|---|---|---|---|---|
| **PS200-RF** | 0.215 ± 0.022 | 2.5 % | 1.05 | 0.68 | Carboxyl | Anionic | 505-545/560-630 |
| **PS2-RF** | 2.0 ± 0.1 | 2.5 % | 1.05 | 0.3 | Carboxyl | Anionic | 505-545/560-630 |

PS200-RF, polystyrene particles of 200 nm; PS2-RF, polystyrene particles of 2 µm

*Cell cultures*

Adherent human epithelial colorectal adenocarcinoma cells (Caco-2; ATCC® HTB-37™, passage 30-40) and human colon adenocarcinoma mucus-secreting cells (HT29-MTX, Sigma Aldrich, Germany, passage 20-30) were cultivated in 75 $cm^3$ culture flasks (Greiner Bio-One International, Austria) containing cell culture medium. Medium was prepared by supplementing Dulbecco's Modified Eagle Medium (DMEM, Sigma-Aldrich, Germany) with 10% heat-inactivated Foetal Bovine Serum (FBS, Sigma-Aldrich, Germany), 1% Penicillin/Streptomycin (P/S, Sigma-Aldrich, Germany), and 1% Minimum Essential Medium of Non-Essential Amino Acids (MEM-NEAA, Sigma-Aldrich, Germany). This medium, further referred to as $DMEM^+$, was refreshed every other day. Cells were incubated at 37°C in a humidified 5% $CO_2$ incubator (Binder Inc., USA), unless indicated otherwise. Cells were subcultured every seven days at 80-90% confluency.

*Physicochemical characterisation of PS MPs*

To determine the effects of the applied cell medium on the diameter and charge of PS MPs, physicochemical characterisation was performed. Particle size was verified with Transmission Electron Microscopy (TEM) (Table 2). Briefly, TEM specimens were prepared using the drop-on-grid method on pioloform-coated 150 mesh copper grids. The grids were treated with Alcian blue to render a positive charge (34). A set of ten TEM micrographs was randomly recorded in bright-field TEM mode using the Philips EM 208 S equipped with a TEM charge-coupled device camera (Morade Soft Imaging System), operating at 60k V. Magnifications in the range of 5600 to 28000 times were selected. Analyses were carried out with ImageJ software. Next, the Zetasizer Ultra-Red (Malvern Panalytical Ltd, UK) was applied to analyse the hydrodynamic size of PS MPs (10mg/ml solution) with the Dynamic Light Scattering (DLS) technique and their surface charge with zeta-potential determination (in a 1mM KCl suspension). These measurements were performed on PS MPs of 200 nm and 2 µm suspended in Milli-Q or $DMEM^+$.

*Quantitative uptake assessment of PS MPs*

Association was quantitatively assessed with either the FLUOstar Omega (BMG Labtech, Germany) or FACSCalibur™ (BD Biosciences, USA) for spectrophotometry and flow cytometry, respectively. For the FLUOstar, black 96-well plates were used for seeding $8.10^4$ cells/well; which were incubated for 5-7 days. After 2 h, 4 h, 8 h, or 24 h of 100 µg/ml PS200-RF exposure in $DMEM^+$, cells were washed (Phosphate Buffered Saline (PBS) + $Ca^{2+}$, $Mg^{2+}$) and measured in PBS (Ex/Em 544/590). For flow cytometry, samples were prepared by detaching the cells from the culture flask similar to subculturing, followed by multiple washing steps in FACS buffer (PBS + 2% FBS). Next, the cells were fixed in 4% Paraformaldehyde (10 min, RT) (Sigma-Aldrich, Germany), pelleted (5 min, 300 g), and washed again with FACS buffer. Samples were preserved in FACS buffer at 4°C. Then, 10 000 gated cells were measured with the FACSCalibur™ (BD Biosciences, USA). Forward scatter was plotted versus side scatter and the percentage of cells associated with red fluorescent PS MPs was consequently determined by plotting the fluorescence (FL2-H) versus cell counts. Percentages were corrected for autofluorescence by subtracting control values.

*Confocal microscopy to study particle association/uptake (Qualitative assessment)*

To generate a confluent monolayer, cells were seeded at a density of $3.10^4$ cells/well on ethanol-sterilized coverslips (24-well plate, VWR International, USA) and cultured for 5-7 days. To generate a differentiated monolayer, cells were seeded ($5.10^4$ cells/well) on transwell inserts (3.0 µm pore size, 1.12 $cm^2$, Corning Costar, USA) and

**Table 2: Characterisation of PS MPs in Milli-Q and DMEM$^+$**

| | TEM | | | DLS | | | | | | | | Z-potential (mv) | | | |
|---|---|---|---|---|---|---|---|---|---|---|---|---|---|---|---|
| | | | | Milli-Q | | DMEM$^+$ (t=2h) | | DMEM$^+$ (t=24h) | | DMEM -FBS (t=24h) | | Milli-Q | DMEM$^+$ (t=2h) | DMEM$^+$ (t-24h) | DMEM -FBS (t-24h) |
| ID | Feret min (µm) | Feret max (µm) | AR | Mean (µm) | PdI | Mean (µm) | PdI | Mean (µm) | PdI | Mean (µm) | PdI | | | | |
| PS2-RF | 2.047 | 2.146 | 1.035 | 1.508 ±0.359 | 0.567 ±0.371 | | | 6.476 ±2.474 | 2.022 ±0.076 | | | -2.96 ±0.49 | | -7.226 ±3.005 | |
| PS200-RF | 0.203 | 0.210 | 1.035 | 0.216 ±0.003 | 0.014 ±0.017 | 0.258 ±0.004 | 0.084 ±0.019 | 0.483 ±0.017 | 0.353 ±0.030 | 0.256 ±0.005 | 0.052 ±0.027 | -40.39 ±0.341 | -13.9 ±1.464 | -41.15 ±4.413 | -24.14 ±0.193 |

TEM: Transmission Electron Microscopy; AR: Aspect Ratio; PS200-RF: polystyrene particles of 200 nm; PS2-RF: polystyrene particles of 2 µm; DLS: Dynamic Light Scattering. DLS and z-potential measurements are represented as ± SD.

cultured for 21 days. To enable visualization of uptake and/or attachment of PS MPs, CellMask Green and Hoechst 33342 stainings (Thermo Fisher Scientific, Canada) were performed to stain the cell membrane and nucleus, respectively. After 2 h, 4 h, 8 h, or 24 h of 100 µg/ml MP exposure, cells were washed once and incubated with 1/250 CellMask Green (5 mg/ml) for 30 min (37°C, dark). Next, cells were washed and fixed with 4% Formaldehyde/PBS (Sigma-Aldrich, Germany) for 10 min (RT). Then, cells were washed again and incubated with 1/1000 Hoechst 33342 (1 mM stock, 10 min, RT). Lastly, the cells were washed and mounted onto a glass slide with the cell layer upwards using Shandon Immu-Mount (Thermo Fisher Scientific, Canada). Slides were left to dry at 4°C in the dark before visualisation with confocal microscopy (LSM900, Zeiss, Germany).

The Laser Scanning Microscopy (LSM) mode was applied with Diode UV (405 nm, 1% power), Diode (488 nm, 1.6% power), and Diode SHG (561 nm, 2% power) lasers. Pinhole size was always set at 1AU and, and the gain equalled 665 v, 645 v, and 873 v for the three lasers, respectively. The 40x water immersion objective created images with a resolution of 512 x 512 pixels. All washing steps were performed with PBS (+$Ca^{2+}$, $Mg^{2+}$). Experiments were conducted in triplicate. Five random sections per experiment were counted manually to obtain a representative particle count. For each section, z-stack images were taken. Using the ZEN-software, the *xyz* acquisition mode was selected to show the complete cell layer. In this mode, an *xy* plane near the middle of the *z*-axis was selected, and the number of cells and total particles were counted on orthogonal views using ImageJ software. Next, a 160 µm trajectory line was scrolled through the *xz* plane to count the number of cells containing particles. Means and standard deviations were determined for each experiment. Additionally, autofluorescence of Caco-2 cells was assessed by visualising unstained cells with confocal microscopy (LSM900, Zeiss, Germany).

*PS MP in vitro transport assessment*

The Millicell® ERS-2 Epithelial Volt-Ohm Meter (Merck Millipore, Germany) was used to measure TEER of cells grown on transwell inserts. After each medium refreshment and before and after PS MP exposure, TEER was determined. This indicated whether the Caco-2 monolayer was intact, and inserts could be considered for experiments (>500 Ω.$Cm^2$). TEER values were also applied to record possible differences in membrane integrity caused by MP exposure. For each measurement, an insert without cells was included as a blank. TEER was then calculated by subtracting the blank and correcting for the inserts growth area.

After 21 days in culture, the differentiated cells were exposed to 100 µg/ml PS200-RF in phenol-free medium (DMEM$^+$ without phenol red). Controls without MPs were included to determine the background signals. Transport of PS MPs was studied using fluorescence intensity measurements (Ex/Em 544/590, FLUOstar Omega, BMG Labtech, Germany) in the basolateral medium. To determine the lower limits of quantification (LLOQ), the standard deviation of five blank values was multiplied by nine. Based on a standard calibration curve of PS MPs in phenol-free medium, the obtained fluorescence intensities were converted to MP concentrations (µg/ml).

*Endocytosis inhibition experiments*

Nystatin inhibits transport by decreasing the amount of cholesterol present in the cell and thus blocking caveolae-mediated endocytosis (active transport). Similar experimental procedures were used as described in '*PS MP in vitro transport assessment*', but a 2 h, 4 h, 8 h, and 24 h 100 µg/ml

PS MP exposure was preceded by 1 h of incubation with 120 u/ml Nystatin (35). Low-temperature incubation (4°C) during 2 h and 4 h of 100 µg/ml PS MP exposure were used to inhibit endocytosis (energy-dependent transport) in general.

*Statistical analysis*

Statistical analysis was performed with GraphPad Prism 5. Results are shown as mean ± SD. Normality was assessed using a Shapiro-Wilk test. Homoscedasticity was determined with Brown-Forsythe and Welch tests. For normally distributed data, either an Unpaired Student's t-test, a two-way ANOVA followed by a Holm-Šidák *post hoc* test, or a one-way ANOVA with Tukey's *post hoc* analysis was applied. For data that was not normally distributed, a Mann-Whitney test was performed. A P-value < 0.05 was considered statistically significant. Each experiment was independent and conducted in triplicate.

## RESULTS

*Characterisation of PS MPs*

Physicochemical properties of MPs affect their interactions with cells. To characterise the MPs, TEM, DLS, and z-potential measurements were carried out (Table 2). TEM results validated the MP sizes provided by the manufacturer. For the 2 µm MPs, TEM measurements showed an average size of 2.097 µm. The 200 nm MPs were found have an average size of 0.207 µm after TEM. Interestingly, we detected an increase in hydrodynamic diameter and PdI after incubation in DMEM$^+$ for both 200 nm and 2 µm particles. The hydrodynamic diameter of PS2-RF went from 1.508 ± 0.359 µm in Milli-Q to 6.476 ± 2.474 µm after 24 h DMEM$^+$ incubation, showing a more than fourfold increase. PdI rose from 0.567 ± 0.371 to 2.022 ± 0.076. However, it should be noted that the PS2-RF MPs approache the limit of the DLS technique. Therefore, these measurements could be erroneous. For the PS200-RF, we measured a more than twofold increase in hydrodynamic diameter from 0.216 ± 0.003 µm in Milli-Q to 0.483 ± 0.017 µm after 24 h in DMEM$^+$. Accordingly, the PdI increased from 0.014 ± 0.017 to 0.353 ± 0.030. Additionally, the z-potential was measured. These results show a decline in z-potential for PS2-RF from -2.96 ± 0.49 mv to -7.226 ± 3.005 mv. PS200-RF first displayed a z-potential rise from -40.39 ± 0.341 mv to -13.9 ± 1.464 mv after 2 h of incubation in DMEM$^+$, followed by a decrease to -41.15 ± 4.413 mv after 24 h of incubation in DMEM$^+$. Lastly, 200 nm MPs were characterised in medium without FBS to determine the influence of serum proteins on the size and charge of MPs. This data displayed a slight increase of 0.04 ± 0.048 µm in hydrodynamic diameter and a rise of 0.038 ± 0.014 in PdI, as well as a z-potential increase to -24.14 ± 0.193 mv following a 24 h incubation period in DMEM-FBS.

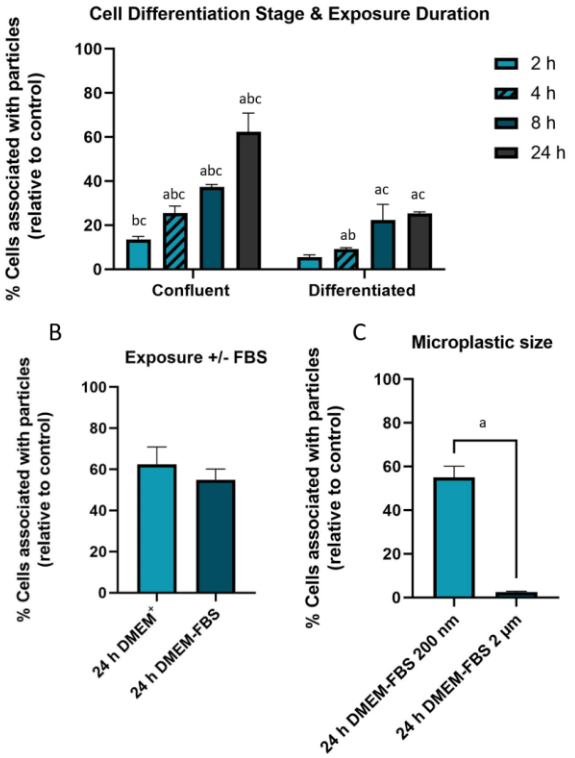


**Figure 2: Quantitative measurements of PS MP association with Caco-2 cells using FACS.** Cells were exposed to 100 µg/ml PS MPs. Percentages were calculated relative to the control (no exposure). **A**. Percentage of confluent and differentiated cells associated (uptake or attachment) with particles after PS200-RF exposure in DMEM$^+$ for 2 h, 4 h, 8 h, or 24 h. **B**. Percentage of confluent cells associated (uptake or attachment) with particles after 24 h PS200-RF exposure in DMEM with or without FBS. **C**. Comparison of percentage of PS200-RF or PS2-RF associated with confluent cells after 24 h DMEM$^+$ exposure. Two way ANOVA, followed by Šidák multiple comparison post hoc analysis (A) or an Unpaired Student's t-test with Welch's correction (B-C) were applied to analyse statistical significance (P < 0.05) a: Significantly different from other exposure condition. b: Significantly different from consequent exposure duration (within an exposure condition). c: Significantly different compared to control (within an exposure condition). Data are represented as mean ± SD.

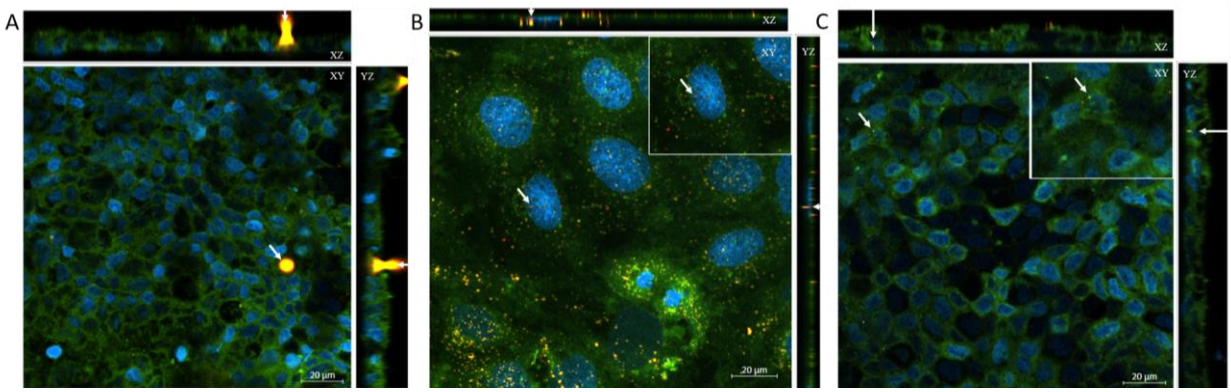


**Figure 3: Orthogonal views of Caco-2 cells stained with CellMask & Hoechst 33342 and exposed to PS2-RF or PS200-RF.** Cells were exposed to 100 µg/ml of either PS200-RF or PS2-RF. **A**. Differentiated Caco-2 monolayer exposed to PS2-RF in DMEM$^+$ for 24 h. **B**. Confluent Caco-2 monolayer exposed to PS200-RF in DMEM$^+$ for 24 h. **C**. Differentiated Caco-2 monolayer exposed to PS200-RF in DMEM$^+$ for 24 h. Nuclei were stained blue using Hoechst 33342, and cell membranes were stained green with CellMask Green. White arrows indicate the presence of red fluorescent PS MP particles (B, C: confirmation of MP internalisation in the cell layer). Images were taken using the Zeiss LSM900 Confocal Microscope at 40X with water immersion.

*Association of PS MPs with an in vitro Caco-2 cell model.*

To quantitatively assess the association (attachment or uptake) of MPs in different exposure conditions, we performed FACS on cells exposed to 100 µg/ml MPs. Firstly, we observed a significant difference in associated PS200-RF between a confluent and differentiated monolayer for multiple exposure durations, i.e., 4 h, 8 h, and 24 h exposure ($P < 0.05$) (Fig. 2A). Secondly, within both the confluent and differentiated monolayer, an increasing trend of associated PS200-RF is observed related to exposure duration. A validation experiment in the confluent monolayer using spectrophotometry confirmed these findings (Fig. S1).

Thirdly, PS200-RF exposures with and without serum proteins were compared, showing that in DMEM-FBS on average 7% less cells were associated with particles, however, these results were not statistically significant (Fig. 2B). Finally, to analyse the effect of MP size on association with the Caco-2 cells, a confluent monolayer was exposed to 100 µg/ml PS200-RF or PS2-RF for 24 h in DMEM$^+$. Significantly more cells were associated with PS200-RF than with PS2-RF ($P < 0.05$) (Fig. 2C).

*Uptake of PS MPs in in vitro Caco-2 models*

MPs uptake was qualitatively determined using confocal microscopy (Fig. 3). Initially, autofluorescence of the Caco-2 cells was tested, which was not observed (Fig. S2). Additionally, staining methods for visualisation of the cell nucleus (Hoechst 33342) and membrane (CellMask Green) were optimized (Fig. S3). By manually counting the cells and particles in z-stack images, a

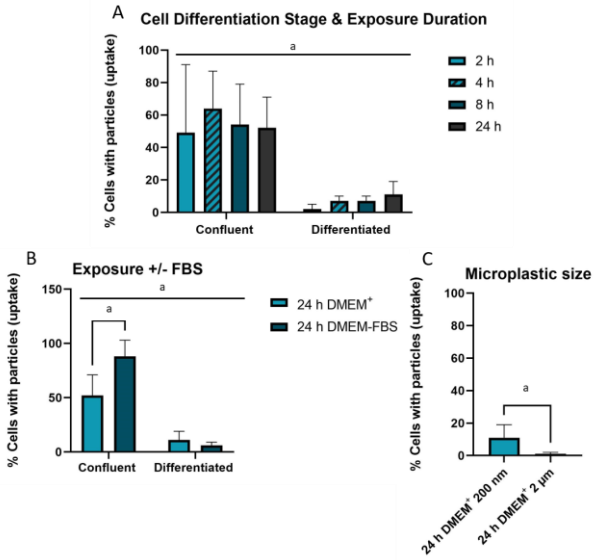


**Figure 4: Uptake of PS MPs in a Caco-2 monolayer using confocal image analysis.** Cells and particles were counted on orthogonal views of confocal images to determine the percentage of cells that internalized a particle compared to the total number of cells visible on the image. Cells were exposed to 100 µg/ml PS MPs. **A**. Percentage of confluent or differentiated cells containing PS200-RF MPs after 2 h, 4 h, 8 h, or 24 h exposure in DMEM$^+$ **B**. Percentage of confluent or differentiated cells containing PS200-RF after 24 h exposure in DMEM with or without FBS. **C**. Comparison of the percentage of differentiated cells containing PS200-RF or PS2-RF MPs after 24 h DMEM$^+$ exposure. Two way ANOVA, followed by Šidák multiple comparison post hoc analysis (A), an Unpaired Student's t-test with Welch's correction (B), or a Mann-Whitney test (C) were applied to analyse statistical significance ($P < 0.05$) a: Significantly different from other exposure condition. Data are represented as mean ± SD.

semi-quantitative result for the percentage of cells that internalized particles compared to all cells present on the image was obtained. We observed a significant difference of on average 48% between the confluent and differentiated monolayer for all exposure durations ($P < 0.05$) (Fig. 4A). These results display similar trends compared to the above-mentioned FACS data (Fig. 2A).

The influence of serum proteins on PS200-RF uptake was tested by comparing exposures in cell medium with and without FBS. Within the confluent monolayer, 36% fewer cells with internalized particles were found after PS200-RF exposure in DMEM medium containing FBS (Fig. 4B). Confocal microscopy images confirmed these findings as more particles were visible in samples without FBS (Fig. S4). Additionally, results differed between the two cell models, with the confluent monolayer displaying significantly more internalisation of PS200-RF than the differentiated monolayer ($P < 0.05$). For the purpose of comparing the uptake of differently sized MPs, the differentiated monolayer was exposed to the same mass concentration of PS200-RF or PS2-RF. We found that larger particles were taken up less by the cells (Fig. 4C).

*Transport of PS200-RF by an in vitro differentiated Caco-2 monolayer*

Besides uptake, the percentage of MP translocation across the cell monolayer relative to the exposure dose was determined. First, we observed transport across the differentiated monolayer of 0.1 - 2.4% for various exposure conditions (Fig. 5). A slightly increasing trend was observed for percentage PS200-RF transport related to exposure duration (Fig. 5A). Second, a pilot experiment showed that inhibiting caveolae-mediated transport with Nystatin resulted in approximately four times more translocation (compared to regular transport of PS200-RF) after 24 h incubation in a differentiated Caco-2 monolayer (Fig. 5A). Comparing inhibition of energy-dependent (active) transport at 4°C in a differentiated Caco-2 monolayer between 2 and 4 h duration resulted in a trend towards less transport of PS200-RF after 4 h of exposure (Fig. 5B). TEER data indicated that the 4 h exposure substantially affected monolayer integrity (Fig. S5). Lastly, transport across a co-culture differentiated monolayer (Caco-2 + HT29-MTX) was compared to the Caco-2 differentiated monolayer. Although no effect on the monolayer TEER integrity was observed (Data not shown), translocation was reduced by more than half in the co-culture differentiated monolayer ($P < 0.05$) (Fig. 5C).

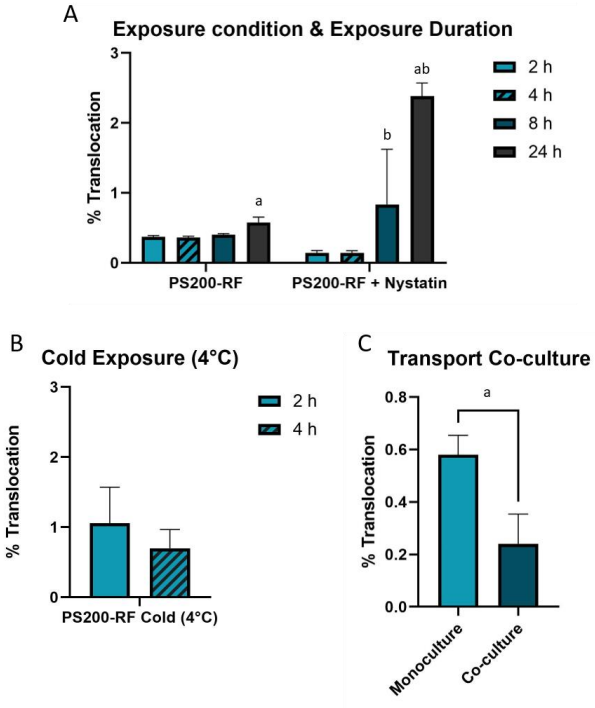


**Figure 5: Transport of PS200-RF by an *in vitro* differentiated Caco-2 monolayer using plate reader-based fluorescence intensity measurements.** Differentiated cells were exposed to 100 µg/ml PS200-RF MPs. Measurements were performed in the basolateral medium. **A**. Percentage of MPs that translocated across the cell monolayer (compared to the total amount added apically during exposure) after 2 h, 4 h, 8 h, or 24 h of exposure. PS200-RF is the control exposure (37°C, 100 µg/ml, PS200-RF). Nystatin was added one hour prior to exposure (37°C, 100 µg/ml, PS200-RF) to inhibit caveolae-mediated endocytosis. **B**. Percentage of PS200-RF that translocated across the cell monolayer (compared to the total amount added apically during exposure) after Cold incubation (4°C) used to inhibit general endocytosis. **C**. Percentage of PS200-RF that translocated (compared to the total amount added apically during exposure) across the Caco-2 cell monolayer and a Caco-2 HT29-MTX co-culture (3:1). Two way ANOVA, followed by Šidák multiple comparison post hoc analysis (A), a Mann-Whitney test (B), or an Unpaired Student's t-test with Welch's correction (C) were applied to analyse statistical significance ($P < 0.05$) a: Significantly different from other exposure condition. b: Significantly different from consequent exposure duration (within an exposure condition). Data are represented as mean ± SD.

## DISCUSSION

Microplastics are important environmental polluters and are found in products that we consume, including seafood, table salt, and even beer (6, 14, 17, 18). One of the major routes of human exposure is ingestion. However, possible

risks to human health are still uncertain (6). This is mostly due to the variety of research methods in existing literature on MP uptake and transport. A lack of fundamental understanding causes difficulties in the interpretation and comparison of the research data. Therefore, we aimed to provide a knowledge basis for the effect of different exposure conditions on PS MP uptake and transport.

The key findings of our study are that uptake and association of PS MPs with the Caco-2 monolayer varied from 1 to 88%, depending on the exposure condition. Association/uptake was found to be influenced by MP size as the PS200-RF were significantly more internalized and associated with the Caco-2 monolayer than PS2-RF. Similar results were found by Wu *et al.*, who observed more MP uptake in Caco-2 cells after exposure to 100 nm PS spheres compared to 5 µm PS spheres via fluorescence microscopy measurements (36). Stock *et al.* found that changes in uptake related to size could be explained by different internalisation mechanisms for differently sized plastics (26). Smaller particles are mainly internalised via caveolae-mediated (± 200 nm) and clathrin-mediated (± 100 nm) mechanisms, while larger particles mostly use alternative transport mechanisms, such as phagocytosis (0.5-10 µm) or macropinocytosis (0.2-5 µm) (26, 37-39). This explains why the Caco-2 cells need more time to internalise 2 µm PS MPs compared to 200 nm PS MPs as uptake mechanisms for larger particles, such as phagocytosis, are generally considered more energy-consuming. However, it is important to state that for both 200 nm and 2 µm plastics, a mass concentration of 100 µg/ml was used. Since these particles differ in size, thousand times fewer PS2-RF MPs were exposed to the Caco-2 cells for the same mass concentration. Additional experiments focussing on MP exposure with a similar number of plastics (different mass concentration) could be interesting to investigate the size effect.

Together with MP size, exposure duration is important to consider when studying MP uptake/association in cells. We determined uptake/association of PS MPs in a Caco-2 monolayer after different exposure durations and stages of cell differentiation (confluent monolayer versus differentiated monolayer). For both the confluent and differentiated cells, FACS results showed that more PS200-RF were associated with the cells after increasing exposure durations. Semi-quantitative uptake analysis using confocal images displayed a similar trend for the differentiated monolayer but not for the confluent monolayer. FACS cannot differentiate between uptake or attachment of PS MPs in cells. The semi-quantitative method was used to assess uptake by the Caco-2 cells exclusively. Therefore, the difference between both results could be due to particle attachment, which was not determined separately. Important to note here is that characterisation our PS200-RF MPs showed a small increase in hydrodynamic diameter after 2 h incubation in $DMEM^+$ and a more than doubling of the hydrodynamic diameter after 24 h in $DMEM^+$. This is possibly due to the formation of a protein corona. Lynch *et al.* demonstrated that plastic particles immediately generate a protein corona upon contact with biological fluids (40, 41). The protein corona has been shown to increase the size of nanoparticles by the formation of multiple protein layers (42). Surprisingly, our uptake results show that the increased hydrodynamic size does not seem to negatively impact uptake related to exposure duration. In fact, we observed an increasing trend for the percentage of Caco-2 cells with PS200-RF uptake/association after prolonged exposure times. However, increasing internalisation and association with longer exposure duration seems intuitive since prolonged exposure gives the cells more time to interact with and internalize particles (20). Additional experiments with longer exposure durations and thorough characterization of the protein corona using SDS-PAGE and proteomics analysis would be of great value.

Our results concerning the effect of serum proteins on MP uptake displayed that confluent cells internalised fewer particles when exposed to PS200-RF in $DMEM^+$ (for 24 h) compared to DMEM-FBS exposure (for 24 h). This decrease in uptake is possibly related to the formation of a protein corona. Due to the presence of serum proteins in medium containing FBS, a protein corona forms on the MPs (43). This was supported by characterisation experiments, where MPs in $DMEM^+$ not only increased in diameter but also in PdI. The increase in diameter, related to the protein corona, could impact uptake since larger size has been shown to affect MP uptake (PS2-RF versus PS200-RF experiment) (44, 45). Additionally, the

rise in PdI after $DMEM^+$ incubation indicates more particle agglomeration of the MPs, which could also be the reason for the observed decrease in uptake (46, 47). Even though the effect is small, incubation in cell medium without proteins (DMEM-FBS) also resulted in a slight increase in hydrodynamic diameter and PdI. This is possibly due to interactions of the negatively charged (carboxylated) MPs with positive ions in the medium and MP agglomeration, respectively (47, 48). From these data, we recommend that the aforementioned interactions and effects should always be taken into account when interpreting experiments on PS MP uptake/association.

When comparing differentiated and confluent monolayers, we observed a significant decrease in both association and uptake of PS200-RF for the differentiated monolayer. Previously, Francia *et al.* demonstrated that 200 nm carboxylated PS MPs entered less HUVEC cells after seven days of differentiation than after three days of differentiation (49). Furthermore, Milovic *et al.* found significantly higher polyamine uptake rates in confluent than in differentiated Caco-2 cells (50). A possible explanation for these results is the area present for MP uptake. In the differentiated monolayer, more cells are present per surface area. Therefore, fewer particles are added per cell in the differentiated monolayer compared to the confluent monolayer, possibly leading to less uptake per cell (which was analysed in this study). These results demonstrate an effect of cell differentiation state on PS MP uptake/association.

After the association and uptake experiments, we analysed PS200-RF transport across a differentiated monolayer. Our results are in line with previous *in vitro* transport studies of Caco-2 cell models, which found a translocation of 0.2 - 10% for varying PS particle sizes and charges (10, 20). Monolayer integrity and the intactness of tight junctions was investigated using TEER measurements. Exposure to 100 µg/ml PS200-RF significantly decreased TEER for all exposure durations. These data suggest an effect of MP exposure on barrier integrity. Therefore, the observed transport could be due to both paracellular (via the tight junctions) and transcellular (endocytosis) transport. Hence, transport mechanisms were the next cellular process we investigated.

Nystatin was applied to inhibit caveolae-mediated endocytosis. Nystatin is a polyene antibiotic that leads to cholesterol depletion within the cell membrane, thereby inhibiting this active transport mechanism (35, 51, 52).

Transport was slightly decreased after 2 h and 4 h of PS200-RF exposure with Nystatin (compared to regular PS200-RF exposure), indicating the effectiveness of this inhibiting agent and the involvement of caveolae-mediated endocytosis. Rejman *et al.* found that 200 nm particles mainly rely on caveolae-mediated transport in mouse melanoma B16 cells (39). To our surprise, we found an increase of percentage translocation after 24 h Nystatin inhibition. This could be due to interference from other transport mechanisms. For example, a rescue mechanism may be activated after prolonged Nystatin inhibition. Alternative transport mechanisms, such as phagocytosis, macropinocytosis or clathrin-mediated transport could be increased in response to declining caveolae-mediated endocytosis (37).

Our co-culture experiments indicated a decrease in overall transport in a co-culture monolayer compared to a monoculture monolayer. These preliminary results show an effect of the presence of mucus on PS200-RF transport, which was also previously observed by other researchers (24, 53). Since monocultures lack this mucus layer, co-culture experiments are especially valuable for charged microplastics due to electrostatic repulsion (10). The PS MPs used in our study are negatively charged as a result of carboxyl groups present on their surface. Since mucus is also negatively charged, it can repulse the carboxylated PS200-RF MPs along with physically decreasing transport by the viscous mucus layer (54). On the contrary, Stock et al. demonstrate more uptake of negatively charged (sulphate or carboxyl groups) PS MPs in a Caco-2 HT29-MTX co-culture compared to a Caco-2 monoculture. However, these results were discovered in MPs of 1 µm and 4 µm, which is much larger than the MPs used in our experiments (26). As previously explained, internalisation and transport mechanisms vary according to MP size. Therefore, these results are not directly comparable to the data from our study. In summary, comparing data between studies should always be performed with care as transport and uptake are largely dependent on cell type, complexity of the model

system, and physicochemical characteristics of the MP (31, 37).

This study has some important strengths. First, we included both confluent and differentiated monolayers. When the cells are differentiated, they become fully functional and possess completely developed tight junctions. Even though the inclusion of a differentiated monolayer slightly increases the complexity of the Caco-2 model system, it still allows for studying specific exposure conditions to gather fundamental knowledge. This would not be possible in more complex models. Additionally, the use of these two cell models facilitates direct comparison between confluent and differentiated monolayers. Second, we included co-culture experiments as well as monoculture data. The use of this co-culture model gives a more realistic image of PS200-RF uptake, therefore increases the reliability of our data. Lastly, we applied multiple methods to assess MP uptake/association with the Caco-2 cells. The combination of FACS, plate reader data, and confocal image analysis provides a comprehensive overview of exposure conditions that affect PS MP uptake and association, such as exposure duration or the presence of serum proteins.

Some limitations regarding this study are acknowledged as well. We used an exposure concentration of 100 µg/ml for all experiments, which is too high to be environmentally relevant. Because low transport rates were expected (10, 20), this high concentration was chosen to be able to quantify transport. Furthermore, it allows for detection of the effects different exposure conditions might have on PS MP uptake and transport, even if these effects are rather small. Furthermore, confocal image analysis was only performed by one person and could thus be prone to bias. This analysis was performed on one slide near the middle of the z-stack rather than all slides; hence results should be regarded as such. Due to time constraints and Covid-19, we were not able to determine cell viability. However, previous experiments from our research group indicated that a PS200-RF exposure concentration of 100 µg/ml did not affect cell viability.

Several future experiments could be interesting as well. The observed increase in hydrodynamic size after $DMEM^+$ incubation along with the rising PS MP uptake/association trend with prolonged exposure indicate an effect of exposure duration and involvement of a protein corona. Therefore, future studies should also include longer and shorter exposure times as well as experiments with DMEM-FBS incubation for varying exposure durations. Some suggestions based on scientific literature are: 10 min, 30 min, 1 h, 48 h, 72 h, and 96 h (20, 21, 36). In addition, uptake and transport experiments with weathered PS MPs or PS MPs that did undergo *in vitro* digestion would be valuable. Microplastics are broken down/weathered by environmental factors (UV radiation, ocean waves etc.) as well as by gastrointestinal juices after ingestion. Previous research has shown that digestive processes lead to a change in physicochemical characteristics of the PS MPs (21). For this reason, experiments with *in vitro* digested and weathered MPs could clarify the influence of the aforementioned processes on MP uptake and transport (55). Finally, endocytosis mechanisms acquire further investigation. As the results of this study are preliminary, we propose additional experiments on the specific endocytosis mechanisms involved in PS200-RF and PS2-RF internalization. First of all, we propose further experimentation with the cholesterol depleting agent Nystatin (to inhibit caveolae-mediated transport). Moreover, experiments using other inhibiting agents, such as chlorpromazine for clathrin-mediated endocytosis and amiloride for micropinocytosis would clarify the role of different endocytosis mechanisms in PS MP uptake and transport. Nonetheless, valuable information was obtained in this study. By enhancing insight into the influence of varying exposure conditions (exposure time, presence of serum proteins, MP size, mucus-producing cells etc.), we provided the information necessary for improved interpretation and comparison of results from MP research.

## CONCLUSION

Taken together, our work presents an overview of the influence of exposure duration, stage of cell differentiation, MP size, and the addition of serum proteins on MP uptake. Furthermore, inhibition of (caveolae-mediated) endocytosis and the presence of mucus-producing cells on MP transport was clarified. This knowledge can be used as a basis for performing, interpreting, and comparing (future) research in this field. However, to fully understand the processes involved in MP uptake and transport,

more research is necessary on physicochemical characterization of MPs, including the protein corona formation, as well as other uptake and transport mechanisms, such as clathrin-mediated endocytosis.

**REFERENCES**


1. Geyer R, Jambeck JR, Law KL. Production, use, and fate of all plastics ever made. Sci Adv. 2017;3(7):e1700782.
2. Barnes DK, Galgani F, Thompson RC, Barlaz M. Accumulation and fragmentation of plastic debris in global environments. Philos Trans R Soc Lond B Biol Sci. 2009;364(1526):1985-98.
3. Erni-Cassola G, Zadjelovic V, Gibson MI, Christie-Oleza JA. Distribution of plastic polymer types in the marine environment; A meta-analysis. J Hazard Mater. 2019;369:691-8.
4. Azevedo-Santos VM, Brito MFG, Manoel PS, Perroca JF, Rodrigues-Filho JL, Paschoal LRP, et al. Plastic pollution: A focus on freshwater biodiversity. Ambio. 2021;50(7):1313-24.
5. Roman L, Hardesty BD, Hindell MA, Wilcox C. A quantitative analysis linking seabird mortality and marine debris ingestion. Sci Rep. 2019;9(1):3202.
6. EFSA. Presence of microplastics and nanoplastics in food, with particular focus on seafood. EFSA Journal. 2016;14(6).
7. Gundogdu S, Yesilyurt IN, Erbas C. Potential interaction between plastic litter and green turtle Chelonia mydas during nesting in an extremely polluted beach. Mar Pollut Bull. 2019;140:138-45.
8. Chapron L, Peru E, Engler A, Ghiglione JF, Meistertzheim AL, Pruski AM, et al. Macro- and microplastics affect cold-water corals growth, feeding and behaviour. Sci Rep. 2018;8(1):15299.
9. Rist S, Baun A, Hartmann NB. Ingestion of micro- and nanoplastics in Daphnia magna - Quantification of body burdens and assessment of feeding rates and reproduction. Environ Pollut. 2017;228:398-407.
10. Walczak AP, Kramer E, Hendriksen PJ, Tromp P, Helsper JP, van der Zande M, et al. Translocation of differently sized and charged polystyrene nanoparticles in in vitro intestinal cell models of increasing complexity. Nanotoxicology. 2015;9(4):453-61.
11. Wright SL, Kelly FJ. Plastic and Human Health: A Micro Issue? Environ Sci Technol. 2017;51(12):6634-47.
12. Sakai-Kato K, Hidaka M, Un K, Kawanishi T, Okuda H. Physicochemical properties and in vitro intestinal permeability properties and intestinal cell toxicity of silica particles, performed in simulated gastrointestinal fluids. Biochim Biophys Acta. 2014;1840(3):1171-80.
13. Cox KD, Covernton GA, Davies HL, Dower JF, Juanes F, Dudas SE. Human Consumption of Microplastics. Environ Sci Technol. 2019;53(12):7068-74.
14. Curren E, Leaw CP, Lim PT, Leong SCY. Evidence of Marine Microplastics in Commercially Harvested Seafood. Front Bioeng Biotechnol. 2020;8:562760.
15. Hernandez LM, Xu EG, Larsson HCE, Tahara R, Maisuria VB, Tufenkji N. Plastic Teabags Release Billions of Microparticles and Nanoparticles into Tea. Environ Sci Technol. 2019;53(21):12300-10.
16. Organization WH. Microplastics in drinking-water. 2019.
17. Liebezeit G, Liebezeit E. Synthetic particles as contaminants in German beers. Food Addit Contam Part A Chem Anal Control Expo Risk Assess. 2014;31(9):1574-8.
18. Yang D, Shi H, Li L, Li J, Jabeen K, Kolandhasamy P. Microplastic Pollution in Table Salts from China. Environ Sci Technol. 2015;49(22):13622-7.
19. Schwabl P, Koppel S, Konigshofer P, Bucsics T, Trauner M, Reiberger T, et al. Detection of Various Microplastics in Human

Stool: A Prospective Case Series. Ann Intern Med. 2019;171(7):453-7.
20. Abdelkhaliq A, van der Zande M, Punt A, Helsdingen R, Boeren S, Vervoort JJM, et al. Impact of nanoparticle surface functionalization on the protein corona and cellular adhesion, uptake and transport. J Nanobiotechnology. 2018;16(1):70.
21. Liu S, Wu X, Gu W, Yu J, Wu B. Influence of the digestive process on intestinal toxicity of polystyrene microplastics as determined by in vitro Caco-2 models. Chemosphere. 2020;256:127204.
22. Walczak AP, Kramer E, Hendriksen PJ, Helsdingen R, van der Zande M, Rietjens IM, et al. In vitro gastrointestinal digestion increases the translocation of polystyrene nanoparticles in an in vitro intestinal co-culture model. Nanotoxicology. 2015;9(7):886-94.
23. Ho BT, Roberts TK, Lucas S. An overview on biodegradation of polystyrene and modified polystyrene: the microbial approach. Crit Rev Biotechnol. 2018;38(2):308-20.
24. Fiorentino I, Gualtieri R, Barbato V, Mollo V, Braun S, Angrisani A, et al. Energy independent uptake and release of polystyrene nanoparticles in primary mammalian cell cultures. Exp Cell Res. 2015;330(2):240-7.
25. Eyles J, Alpar O, Field WN, Lewis DA, Keswick M. The transfer of polystyrene microspheres from the gastrointestinal tract to the circulation after oral administration in the rat. J Pharm Pharmacol. 1995;47(7):561-5.
26. Stock V, Bohmert L, Lisicki E, Block R, Cara-Carmona J, Pack LK, et al. Uptake and effects of orally ingested polystyrene microplastic particles in vitro and in vivo. Arch Toxicol. 2019;93(7):1817-33.
27. Angelis ID, Turco L. Caco-2 cells as a model for intestinal absorption. Curr Protoc Toxicol. 2011;Chapter 20:Unit20 6.
28. Hubatsch I, Ragnarsson EG, Artursson P. Determination of drug permeability and prediction of drug absorption in Caco-2 monolayers. Nat Protoc. 2007;2(9):2111-9.
29. Jumarie C, Malo C. Caco-2 cells cultured in serum-free medium as a model for the study of enterocytic differentiation in vitro. J Cell Physiol. 1991;149(1):24-33.
30. He B, Lin P, Jia Z, Du W, Qu W, Yuan L, et al. The transport mechanisms of polymer nanoparticles in Caco-2 epithelial cells. Biomaterials. 2013;34(25):6082-98.
31. Stock V, Laurisch C, Franke J, Donmez MH, Voss L, Bohmert L, et al. Uptake and cellular effects of PE, PP, PET and PVC microplastic particles. Toxicol In Vitro. 2021;70:105021.
32. Wang Q, Bai J, Ning B, Fan L, Sun T, Fang Y, et al. Effects of bisphenol A and nanoscale and microscale polystyrene plastic exposure on particle uptake and toxicity in human Caco-2 cells. Chemosphere. 2020;254:126788.
33. Kulkarni SA, Feng SS. Effects of particle size and surface modification on cellular uptake and biodistribution of polymeric nanoparticles for drug delivery. Pharm Res. 2013;30(10):2512-22.
34. Jan Mast EV, Vasile-Dan Hodoroaba, Ralf Kaegi. Chapter 2.1.2 - Characterization of nanomaterials by transmission electron microscopy: Measurement procedures. In: Vasile-Dan Hodoroaba WESU, Alexander G. Shard, editor. Characterization of Nanoparticles: Elsevier; 2020. p. 29-48.
35. Lewis SA, Eaton DC, Clausen C, Diamond JM. Nystatin as a probe for investigating the electrical properties of a tight epithelium. J Gen Physiol. 1977;70(4):427-40.
36. Wu B, Wu X, Liu S, Wang Z, Chen L. Size-dependent effects of polystyrene microplastics on cytotoxicity and efflux pump inhibition in human Caco-2cells. Chemosphere. 2019;221:333-41.
37. Tore-GeirIversen TS, Kirsten Sandvig. Endocytosis and intracellular transport of nanoparticles: Present knowledge and need for future studies. Nanotoday. 2011;6(2):176-85.
38. Yue-Xuan Li H-BP. Macropinocytosis as a cell entry route for peptide-functionalized

and bystander nanoparticles. Journal of Controlled Release. 2021;329:1222-30.
39. Rejman J, Oberle V, Zuhorn IS, Hoekstra D. Size-dependent internalization of particles via the pathways of clathrin- and caveolae-mediated endocytosis. Biochem J. 2004;377(Pt 1):159-69.
40. Iseult Lynch CW, Eugenia Valsami-Jones. A strategy for grouping of nanomaterials based on key physico-chemical descriptors as a basis for safer-by-design NMs. Nano Today. 2014;9(3):266-70.
41. Dell'Orco D, Lundqvist M, Oslakovic C, Cedervall T, Linse S. Modeling the time evolution of the nanoparticle-protein corona in a body fluid. PLoS One. 2010;5(6):e10949.
42. Jiang X, Weise S, Hafner M, Rocker C, Zhang F, Parak WJ, et al. Quantitative analysis of the protein corona on FePt nanoparticles formed by transferrin binding. J R Soc Interface. 2010;7 Suppl 1:S5-S13.
43. Shruti R Saptarshi ADALL. Interaction of nanoparticles with proteins: relation to bio-reactivity of the nanoparticle. Journal of Nanobiotechnology. 2013;11(26).
44. Guarnieri D, Guaccio, A., Fusco, S., & Netti, P. A. Effect of serum proteins on polystyrene nanoparticle uptake and intracellular trafficking in endothelial cells. . Journal of Nanoparticle Research. 2011;30(9):4295–309.
45. Tenzer S, Docter D, Kuharev J, Musyanovych A, Fetz V, Hecht R, et al. Rapid formation of plasma protein corona critically affects nanoparticle pathophysiology. Nat Nanotechnol. 2013;8(10):772-81.
46. Thilak Mudalige HQ, Desiree Van Haute, Siyam M. Ansar, Angel Paredes, Taylor Ingle. Characterization of Nanomaterials: Tools and Challenges. Nanomaterials For Food Applications2019. p. 313-53.
47. Bruinink A, Wang J, Wick P. Effect of particle agglomeration in nanotoxicology. Arch Toxicol. 2015;89(5):659-75.
48. Sabuncu AC, Grubbs J, Qian S, Abdel-Fattah TM, Stacey MW, Beskok A. Probing nanoparticle interactions in cell culture media. Colloids Surf B Biointerfaces. 2012;95:96-102.
49. Francia V, Aliyandi A, Salvati A. Effect of the development of a cell barrier on nanoparticle uptake in endothelial cells. Nanoscale. 2018;10(35):16645-56.
50. Vladan Milovic MD MSc DFM, Lyudmila Turchanowa PhD, Jürgen Stein MD PhD, Wolfgang F Caspary MD. Permeability Characteristics of Polyamines Across Intestinal Epithelium Using the Caco-2 Monolayer System: Comparison BetweenTransepithelial Flux and Mitogen-Stimulated Uptake Into Epithelial Cells. Basic nutritional investigation. 2001;17(6):462-6.
51. Ivanov AI. Pharmacological inhibition of endocytic pathways: is it specific enough to be useful? Methods Mol Biol. 2008;440:15-33.
52. Gitrowski C, Al-Jubory AR, Handy RD. Uptake of different crystal structures of TiO(2) nanoparticles by Caco-2 intestinal cells. Toxicol Lett. 2014;226(3):264-76.
53. Sato K, Nagai J, Mitsui N, Ryoko Y, Takano M. Effects of endocytosis inhibitors on internalization of human IgG by Caco-2 human intestinal epithelial cells. Life Sci. 2009;85(23-26):800-7.
54. Norris DA, Puri N, Sinko PJ. The effect of physical barriers and properties on the oral absorption of particulates. Adv Drug Deliv Rev. 1998;34(2-3):135-54.
55. Versantvoort CH, Oomen AG, Van de Kamp E, Rompelberg CJ, Sips AJ. Applicability of an in vitro digestion model in assessing the bioaccessibility of mycotoxins from food. Food Chem Toxicol. 2005;43(1):31-40.

*Acknowledgements* – DS thanks Dr. Nelly Saenen, Prof. Dr. Karen Smeets, and Msc. Margo Witters for the critical remarks, feedback and guidance. The authors acknowledge the Centre for Environmental Sciences (CMK) for providing access to the labs and equipment. A word goes to Dr. Frank Van Belleghem for providing TEM images and to Meriam Boulik for aiding with the DLS and z-potential measurements. DS would like to gratefully acknowledge Prof. Dr. Anitha Ethirajan for following the progress of this internship and giving valuable advice. Lastly, DS is grateful to Prof Dr. Karen Smeets and Dr. Nelly Saenen for the opportunity to grow and learn within this research group.

*Author contributions* – NS, AE, and KS conceived and designed the research. DS, MW, and NS executed experiments. DS performed the data analysis. FVB and MB provided assistance with TEM images and DLS measurements, respectively. DS wrote the paper. All authors carefully edited the manuscript.

**Max. 25 pages with figures/tables (excluding supplementals)**
**Deadline of submission: 10/06/2021**

## SUPPLEMENTARY INFORMATION

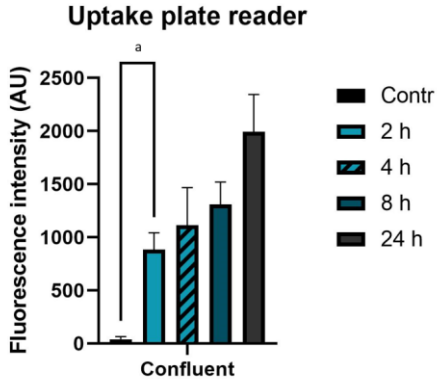


**Figure S1: Quantitative uptake measurements of PS200-RF in a confluent Caco-2 monolayer using plate reader-base fluorescence intensity measurements.** Confluent cells were exposed to 100 µg/ml PS200-RF MPs. After washing the cells twice with PBS, fluorescence was measured at Ex/Em 540-590. A Brown-Forsythe and Welch one way ANOVA followed by Tukey's *post hoc* test was applied to analyse statistical significance ($P < 0.05$). a: Significantly different from other exposure condition. Data are represented as mean ± SD.

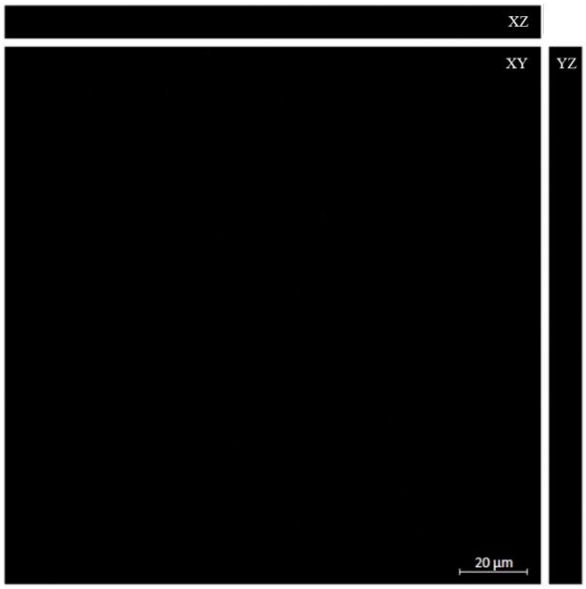


**Figure S2: Orthogonal view of unstained Caco-2 cells to assess autofluorescence.** Images were taken using the Zeiss LSM900 Confocal Microscope at 40X with water immersion.

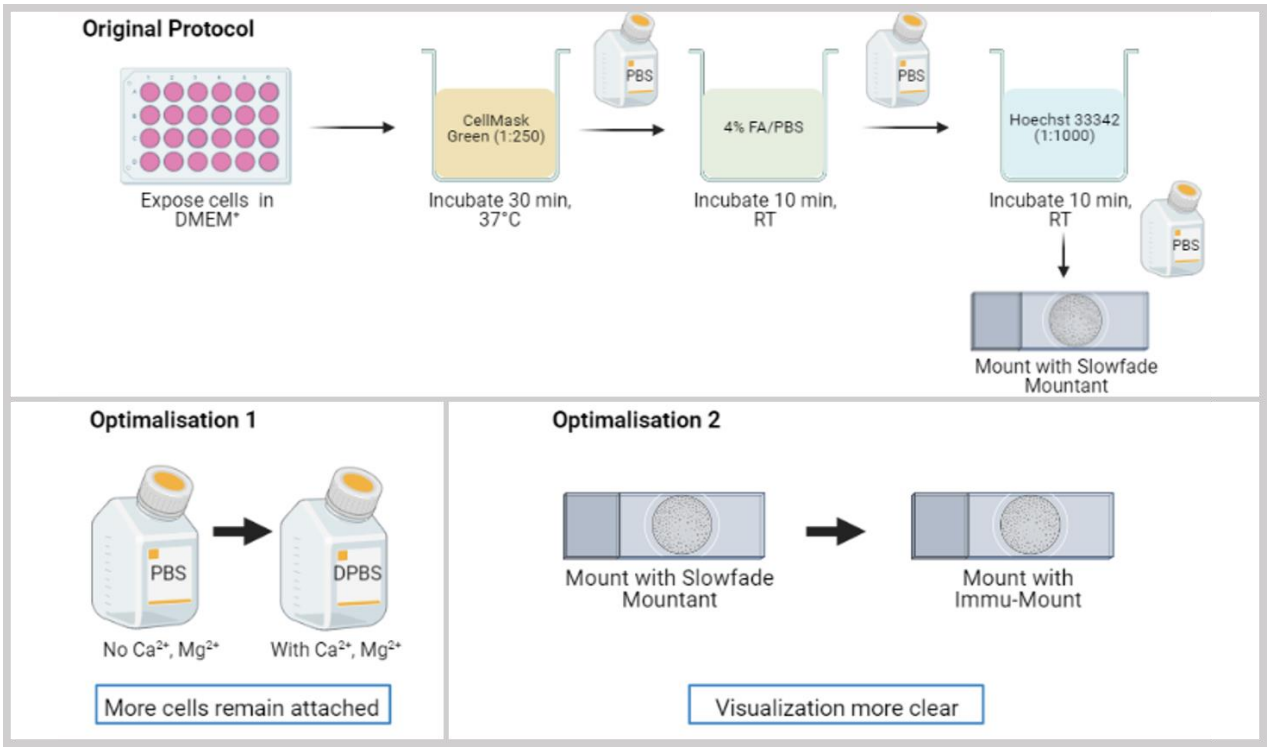


**Figure S3: Optimalization procedure for the CellMask & Hoechst 33342 staining for cell membrane and nucleus, respectively.** Washing steps with PBS (no $Ca^{2+}$, $Mg^{2+}$) were replaced by washing steps using PBS with $Ca^{2+}$and $Mg^{2+}$ to overcome detatching of the cells. Cells were mounted onto a glass slide using Immu-Mount instead of Slowfade Mountant for a more clear image.

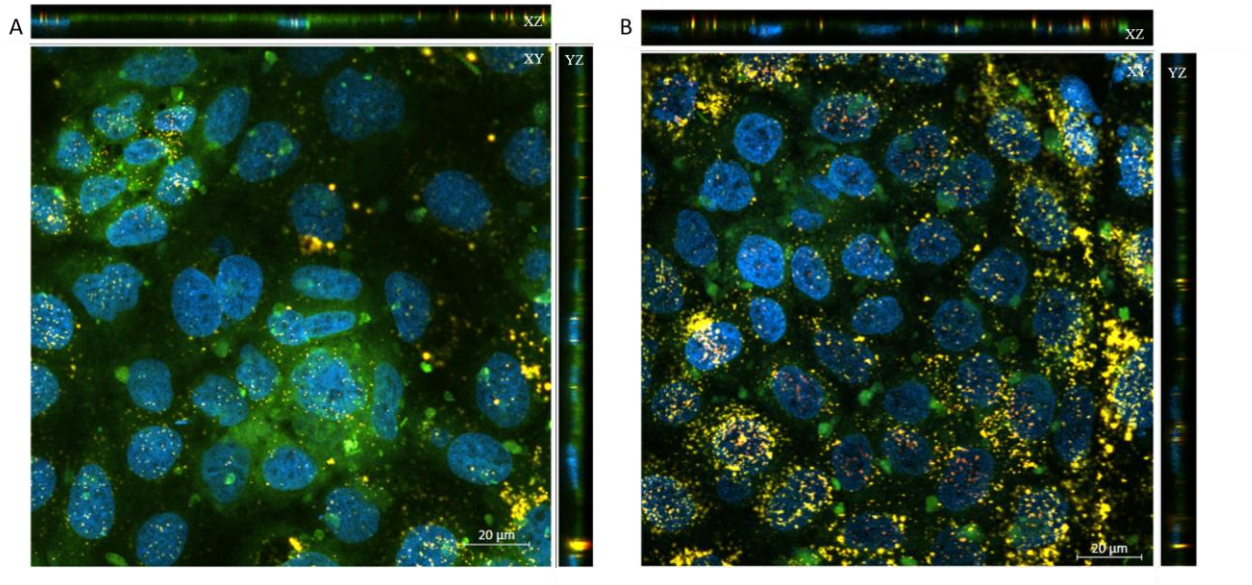


**Figure S4: Orthogonal views of Caco-2 cells stained with CellMask & Hoechst 33342 and exposed to PS200-RF. A**. Confluent Caco-2 cells exposed to 100 µg/ml PS200-RF in $DMEM^{+}$ for 24 h. **B**. Confluent Caco-2 cells exposed to 100 µg/ml PS200-RF DMEM-FBS for 24 h. Nuclei were stained blue using Hoechst 33342 and cell membranes were stained green with CellMask Green. Images were taken using the Zeiss LSM900 Confocal Microscope at 40X with water immersion.

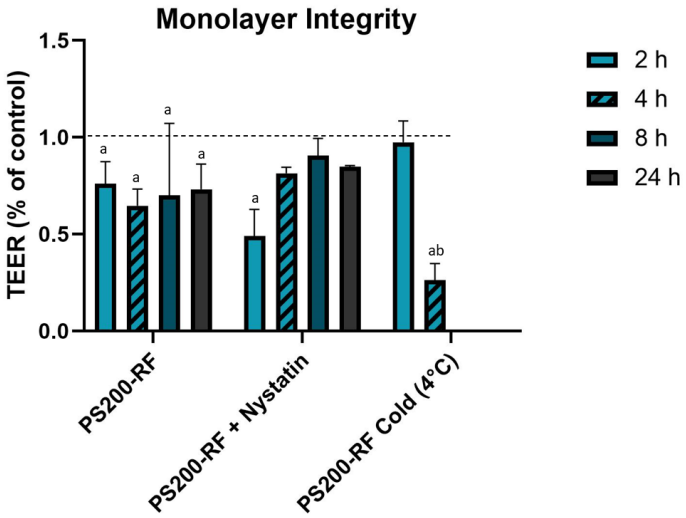


**Figure S5: Transepithelial electrical resistance (TEER) data in percentage of control.** TEER was measured with each change of cell medium and before and after 2 h, 4 h, 8 h and 24 h of PS200-RF exposure in $DMEM^+$ using a Millicell® ERS-2 Epithelial Volt-Ohm Meter. Statistical significance was analysed with a Two-way ANOVA, followed by Holm-Šidák multiple comparison post hoc analysis ($P < 0.05$). a: Significantly different from control (before exposure) b: Significantly different from PS200-RF. Data are represented as mean ± SD